Capillary forces in a confined isotropic-nematic liquid crystal

A. Borštnik Bračič
Faculty of Education, University of Ljubljana, Kardeljeva ploščad 16, 1000 Ljubljana, Slovenia
and Primorska Institute for Natural Sciences and Technology, C. Marežganskega upora 2, 6000 Koper, Slovenia

K. Kočevar
J. Stefan Institute, Jamova 39, 1000 Ljubljana, Slovenia

I. Muševič* and S. Žumer
Faculty of Mathematics and Physics, University of Ljubljana, Jadranska 19, 1000 Ljubljana, Slovenia
and J. Stefan Institute, Jamova 39, 1000 Ljubljana, Slovenia
(Received 20 February 2003; published 28 July 2003)

We have investigated nematic capillary condensation in the isotropic phase of nematic liquid crystals 5CB (4-cyano-4′-*n*-pentylbiphenyl) and 8CB (4-cyano-4′-*n*-octylbiphenyl) confined to nanometer thick layers between two orienting surfaces. The capillary condensation was induced by decreasing the liquid crystal layer thickness using an atomic force microscope, and the onset of condensation was detected by monitoring the structural force on a confining surface. Very strong and long-ranged capillary forces were observed at temperatures close to the isotropic-nematic transition. We have analyzed the temperature dependence of the thickness of the liquid crystal layer, at which the condensation occurs, with a thermodynamic Kelvin equation and determined the interfacial tension between the isotropic and nematic phases. The separation dependence of capillary forces was analyzed within the Landau–de Gennes approach, including electrostatic interaction due to surface charging. The quantitative agreement between the measured and calculated force profiles is very good, and a single set of parameters is needed to describe a set of measured force profiles at different temperatures. Surface charge density, surface potential, and Debye screening length were determined directly from the observed surface forces.

DOI: 10.1103/PhysRevE.68.011708 PACS number(s): 61.30.Hn, 68.08.−p, 61.30.Pq, 68.08.Bc

I. INTRODUCTION

Capillary condensation is a well known phenomenon where a phase transition from a less ordered phase to a more ordered phase is caused by confinement. It is most commonly encountered in the case of water, where water vapor spontaneously condenses in narrow cracks and pores with hydrophilic surfaces. The condensed water forms microscopic capillary bridges between confining surfaces, and the resulting capillary force due to surface tension contributes importantly to the cohesion and adhesion of soil, concrete, and other porous media. It can cause deformation of the solid phase, shrinkage and even cracking [1]. The capillary condensation of water in pores and cracks was described thermodynamically in 1871 by Kelvin [2].

The phenomenon can be found in any system that exhibits first-order phase transition. For a nematic liquid crystal, it was predicted in 1976 by Sheng [3]. Just like water vapor condenses in a gap between hydrophilic surfaces, the isotropic (disordered) liquid crystal condenses into a nematic phase (ordered) in the slit of thickness d between surfaces that tend to align liquid crystal. This condensation into a more ordered phase occurs at temperatures higher than the bulk transition temperature. The phase transition line of capillary condensation is of first order, and it was predicted that the line of capillary phase transition ends in a critical point (d_K, T_K) in a (d,T) phase diagram [3–5].

An important manifestation of the capillary condensation phenomenon is that it exerts forces on the surfaces, between which the condensate forms. Since the surfaces between which the capillary condensation occurs prefer the more ordered phase, the surface contact angle of the interface between the less ordered and more ordered phases is less than 90°. As a consequence, a concave meniscus of the condensed phase is formed between the confining surfaces and a Laplace pressure across this curved meniscus pulls the surfaces together. Capillary condensation therefore results in an attractive force between confining surfaces. The phenomenon of capillary condensation is obviously interesting not only from the fundamental point of view, but it also addresses a more general question of rheological and wetting properties of few-nm-thin layers of complex fluids. The structural force due to capillary condensation of a complex fluid between microscopic objects could also be used for a simple temperature control of forces that could determine the structure and stability of liquid crystal emulsions and dispersions with remarkable optical properties [6–10].

In spite of the great importance of surface and interfacial properties of liquid crystals, the surface-induced spontaneous capillary condensation in nematics remained unobserved until our recent atomic force microscope (AFM) experiment [11]. Several attempts to determine the line of the nematic capillary phase transition using ellipsometry, light scattering, and NMR [12–18] failed, as the shift of the temperature of spontaneous capillary condensation with decreasing thickness of the sample is very small, i.e., 10^{-2} K for a film of 1 μm thickness and becomes significant for surface separations smaller than 100 nm.

*Email address: igor.musevic@ijs.si

Following phenomenological predictions for the pretransitional behavior of the structural forces in thin nematic films, we have recently shown [11] that nematic capillary condensation can be studied with unprecedented accuracy using a temperature controlled AFM. In our previous paper [11], we have focused on the shape of the capillary phase transition line and the location of the critical point (d_K, T_K) in a (d,T) phase diagram. We have found good agreement between the experimentally determined phase diagram and the Landau–de Gennes theory of surface-induced order in an isotropic phase of a nematic liquid crystal. In this paper we describe the AFM experiments in more detail and concentrate on the quantitative analysis of the separation dependence of the capillary force and its temperature evolution. In the experimental part, we describe materials and experimental methods, which is followed by the presentation of force-versus-separation data at different temperatures and for different combinations of liquid crystalline materials and surfaces. In the theoretical part, we describe the Landau–de Gennes mean field formalism of liquid crystal mediated interactions between surfaces. We also consider the electrostatic interaction between surfaces, which was also observed in the experiments. The paper is concluded by comparison of experiment and theory.

II. EXPERIMENT

A. Materials and methods

There are two important experimental issues that have to be precisely controlled in order to observe the nematic capillary condensation in a confined nematic sample: (i) good control of the temperature of the liquid crystal sample (of the order of 1 mK), and (ii) precise control (1 nm) of the separation between the surfaces that confine and orient the liquid crystal. Since it is experimentally practically impossible to align two parallel flat plates at 1 nm separation, curved surfaces are used instead. In our case, one of the confining surfaces was a glass sphere of a radius of the order of ≈ 10 μm, which is much larger than a typical separation between the surfaces (≈ 10 nm) and the other surface was a flat glass or sapphire plate.

In our study of the capillary condensation we have used an AFM (Nanoscope III, Digital Instruments), equipped with a double temperature control as schematically presented in Fig. 1. The microscope was used in the force spectroscopy mode, where the force on the cantilever was measured during approaching or retracting from the surface. The glass sphere was attached to the cantilever, so that the force between the flat substrate and a microsphere was measured as a function of surface separation. Using AFM, it is possible to control the separation between the sphere and the substrate with a sub-nanometer precision. Our design of the double heater enabled us to control the temperature with a precision of 0.01 K. The temperature gradient across the liquid crystal was of the order of ≈ 1 K/mm. We have used nematic liquid crystals 4-cyano-4′-*n*-octylbiphenyl (8CB) and 4-cyano-4′-*n*-pentylbiphenyl (5CB), as obtained from Merck (Germany). Both liquid crystals exhibit isotropic to nematic phase transition, 5CB at 36 °C and 8CB at 41 °C.

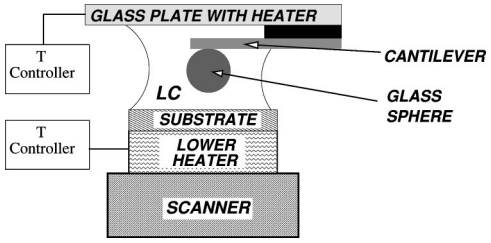

FIG. 1. The schematic representation of the experimental setup used in our experiments. A glass sphere of diameter ≈ 10 μm was attached to the AFM cantilever. Liquid crystal fills the gap between the substrate and the upper glass plate with an integrated heater. An additional heater is mounted between the piezoscanner and the substrate. Both heaters are connected to two independent temperature controllers. Note that the size of the glass sphere is highly exaggerated.

The experiments have been performed on various substrates: BK7 glass (Donnelly PD5005/5088) and sapphire (Edmund Scientific) plates have been used as substrates, attached to the lower heater of the atomic force microscope. BK7 glass microspheres have been glued to the atomic force microscope cantilever, as described elsewhere. The substrates as well as the glass spheres were cleaned in an ultrasonic laboratory detergent bath, rinsed with distilled water, and additionally cleaned with oxygen radio-frequency plasma. After the cleaning procedure, the substrates and glass spheres, already glued to the AFM cantilevers, have been coated with a monolayer of *N,N-dimethyl-N-octadecyl-3-aminopropyltrimethoxysilyl chloride* (DMOAP) (ABCR, Germany). The glass substrates and mounted glass spheres were left in a 1% DMOAP solution for 10 min. Fresh DMOAP solution was used each time the experiment was performed. After the deposition process, the cantilevers with mounted spheres and substrates were thoroughly cleaned in distilled water to remove the excess surfactant from the surfaces. Finally, they have been dried at 110 °C for 1.5 h.

The DMOAP coating is known to produce strong and stable homeotropic alignment of cyanobiphenyl liquid crystals [19,20]. DMOAP monomers adsorb chemically on the glass substrate by forming the hydrogen bond between hydrolyzed methoxysilane group and hydrophilic glass surface [21]. In addition, the DMOAP monomers polymerize during drying and heating, which stabilizes the coating further [21]. The resulting DMOAP monolayer consists of short propyl $[(CH_2)_3]$ chains in the plane of the substrate and octadecyl hydrocarbon chains $(C_{18}H_{37})$, stretching perpendicularly from the surface. These chains are able to interact with liquid crystal molecules and orient these parallel to them, thus enforcing the homeotropic alignment of the liquid crystal [21,22]. We have checked the orientation of the liquid crystal sample between two silane covered glass plates under the polarizing microscope and found perfect homeotropic orientation of the nematic liquid crystal.

During the force experiments, we have found that the cleaning procedure is the most important step in the experimental preparation, since no capillary condensation has been observed, when the surfaces have not been cleaned in the

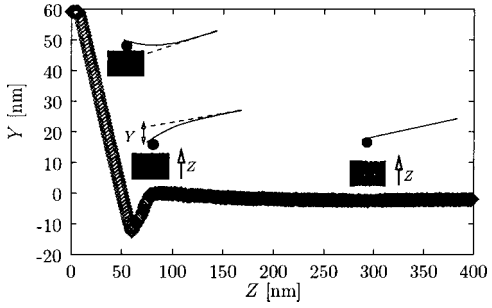

FIG. 2. A typical force curve, recorded with an AFM. The DMOAP coated glass sphere is approached to the DMOAP coated flat glass substrate. A long-range repulsion is seen in this particular case, followed by a region of attraction. The steep, linearly sloped region indicates the hard mechanical contact between the substrate and the sphere. From the slope of the line in this region, the cantilever deflection and the zero of separation are determined. Z denotes the piezotravel and Y is for deflection of the cantilever.

oxygen plasma. We conjecture that the organic contaminants on the glass surface prevent the homogeneous coverage of the surface with the DMOAP layer. Decreased surface density of DMOAP leads to a smaller mesoscopic surface coupling energy and prevents the occurrence of condensation.

B. Measurements and observations

In our study, the atomic force microscope has been used in the force spectroscopy mode. In this mode of operation, the flat surface of the sample is periodically approached and retracted to the glass sphere mounted on the elastic cantilever. The deflection of the cantilever, which measures the net force between the glass sphere and the flat substrate, is simultaneously recorded. As a result, a ''force plot,'' which represents the dependence of the cantilever deflection on the piezo vertical movement, is obtained. A typical force plot from our experiments is shown in Fig. 2.

The deflection of the cantilever is calibrated from the part of the force plot where surfaces of the sphere and the substrate are in contact. This corresponds to the linear region at the left side of Fig. 2. In this region, the deflection of the cantilever is equal to the piezo movement, which is used as a reference for the calibration of deflection. Next, we converted the ''deflection-piezo-travel distance'' curves to the force versus separation curves. The force is obtained from deflection of cantilever Y, multiplied by an elastic constant k, which is specific to a cantilever. Separation is obtained with a simple transformation $d=Z+Y-of$, where d is the separation between the surfaces, Z is the position of the piezo and of is the offset of the piezo-zero-position with respect to the zero of separation, determined from the position of the hard contact. Based on our previous studies of cyanobiphenyl-DMOAP studies, we know that at $d=0$ the glass sphere and the substrate are still not in contact, since there are still adsorbed layers of liquid crystal molecules and DMOAP alkyl chains on each surface, forming the gap of $\approx 5-6$ nm between both bare surfaces. These adsorbed layers cannot be squeezed out of the gap between the two surfaces, as the pressure available in the experiments with a microsphere is

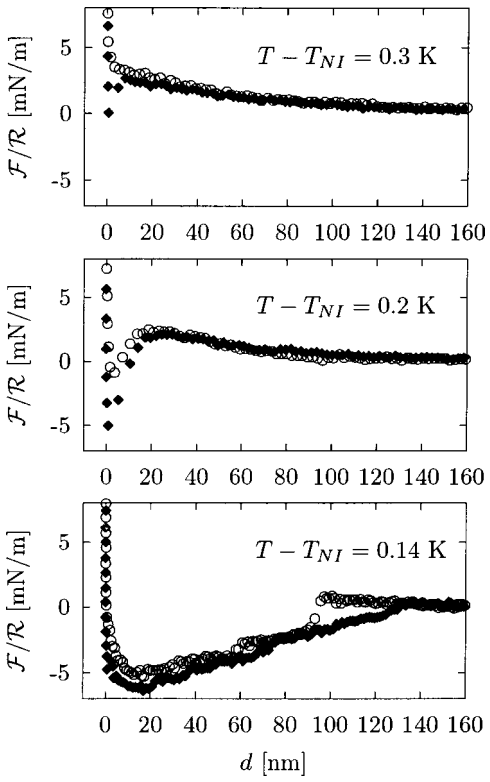

FIG. 3. Force $\mathcal{F}$ normalized with radius of the sphere $R=10\ \mu$m versus separation d between the surfaces in 8CB at different temperatures close to the phase transition temperature T_{NI}. Circles represent force on approach and diamonds force on retraction.

orders of magnitude too small, as we have reported in our previous paper [19,20]. In our experiment, this is actually an advantage, since the van der Waals force is quite small at this distance of separation and so it does not contribute much to the adhesion between the surfaces [1].

Force curves were collected by first setting the temperature of the liquid crystal sample, waiting for the temperature to stabilize, and then recording several force curves at a given temperature. Typically, the speed of piezo movement was of the order of 200 nm/s. At this speed, viscous forces could not be detected and were neglected in our analysis.

In Fig. 3 we present measured forces between the 10-μm DMOAP coated glass sphere and DMOAP coated glass substrate in 8CB at different temperatures above the isotropic to nematic phase transition temperature T_{NI}. At a temperature of 0.3 K above the T_{NI}, we observe a long-ranged repulsive force. As this repulsion is temperature independent and falls exponentially with increasing separation, we conclude that this is simply a screened double layer electrostatic interaction, which we have reported before [23]. After lowering the temperature only slightly ($T-T_{NI}=0.2$ K on Fig. 3), one can clearly observe the appearance of an additional attractive force, which appears at a separation of $d_{cap}=15$ nm. When the temperature is further lowered toward the bulk phase transition temperature T_{NI} (the lowest force plot in Fig. 3), the separation d_{cap} increases strongly and becomes very large (i.e., micrometer scale) close to the phase transition. By

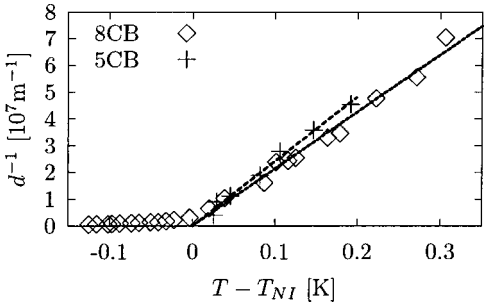

FIG. 4. The temperature dependence of the inverse surfaces separation, where the capillary condensation occurs d_{cap}^{-1}.

precisely lowering the temperature, we were able to follow the increase of the separation d_{cap} up to even more than 1 μm.

One can clearly see from the presented force plots that there is clearly a certain ''critical'' separation, where there is a sudden increase of the attractive force. This attractive force then gradually increases when the separation between both surfaces is further decreased.

It is quite evident that the observed attractive force cannot be attributed to the classical physical forces between the surfaces (electrostatic force, van der Waals force), since (i) these do not depend critically on the temperature and (ii) their separation dependence is monotonic, and there can be no discontinuous increase in force at a certain separation. Rather than that, the observed force is clearly a kind of a structural force related to the phase transition in a liquid crystal. The magnitude of the observed force and its sudden appearance suggest that it might be the capillary force due to nematic condensation in a thin layer of an otherwise isotropic liquid crystal. As a consequence of condensation, a capillary bridge is formed between the two surfaces, which pulls them together.

Additional evidence for the interpretation of the observed force as a capillary condensation is given by the temperature dependence of the distance d_{cap}. It is presented for 5CB and 8CB in Fig. 4. It can be seen from Fig. 4 that the relation between the inverse of d_{cap} and $T-T_{NI}$ is almost linear. This is in agreement with the predictions by Kelvin [2]. His equation for the capillary condensation explains the dependence of the pore size, where a capillary condensation occurs, on the partial pressure of water vapor. With some assumptions, the equation can be rewritten for the case of a nematic liquid crystal [5], $1/d_{cap}=(h_N/2\gamma\cos\Theta)(\Delta T/T_{NI})$, where γ is the interfacial tension between the nematic and isotropic phases, respectively, Θ is the contact angle between both phases on the third (solid) phase, ΔT is the shift of the phase transition temperature, and h_N is the enthalpy of the isotropic-nematic phase transition. The contact angle describes the affinity of the substrate for each of the phases and is 0 if the surface is completely wet by the nematic phase and π if the surface prefers isotropic phase over nematic phase. Since enthalpies of the isotropic-nematic phase transition in 5CB and 8CB are well known (1.56×10^6 Jm^{-3} and 2.37×10^6 Jm^{-3} [24,25]), the slope of the line in $[d_{cap}^{-1},(T-T_{NI})]$ is directly related to the interfacial tension between the isotropic (analog to the vapor) and nematic (analog to liquid) phases. The analysis of the phase diagram, presented in Fig. 4, gives us the product of the interfacial tension and the cosine of the contact angle $\gamma_{NI}\cos\Theta$, which are collected in Table I for 5CB and 8CB on the silanated glass surfaces. The isotropic-nematic interfacial tension is therefore of the order of 1.0×10^{-5} Jm^{-2} if the complete wetting of the substrate with a nematic phase is assumed. This is in agreement with the existing data [26,27] and represents a direct proof that the observed attractive force is due to surface-induced capillary condensation of a nematic phase.

TABLE I. Product of the interfacial tension and cosine of the contact angle of the nematic-isotropic interface for 5CB and 8CB, as obtained from the temperature dependence of the thickness, where the capillary force is observed. The inverse thickness was plotted against the temperature shift and fitted to the Kelvin equation (Fig. 4).

Liquid crystal	$\gamma_{NI}\cos\Theta$ [Jm^{-2}]
5CB	$1.0\times10^{-5}(1\pm0.1)$
8CB	$1.78\times10^{-5}(1\pm0.15)$

III. CALCULATION OF FORCES MEDIATED BY THIN LIQUID CRYSTAL FILMS AT TEMPERATURES ABOVE THE NEMATIC-ISOTROPIC PHASE TRANSITION

A. Description of model structure

In our experiment the interaction between few micrometers sized sphere and a flat surface is mediated by a liquid crystal film with thickness that is small compared to the diameter of the sphere. The experiments indicate that capillary condensation occurs gradually, starting in the region of the smallest thickness and then in other areas. As surfaces are not perfect, a certain degree of randomness is expected in conditions for the local capillary condensation. This is clearly proved by the existence of irregular steps in the force-versus-separation plots (Fig. 3). We therefore propose a model structure, where the surface of the spherical particle is approximated by several conical areas whose cross sections in any plane containing the axis of symmetry are polygons of N equally long line segments (see Ref. [9]). The volume between the flat surface and the sphere is divided into a large number of concentric regions as shown in Fig. 5, and capillary condensation occurs when local conditions for the transitions are satisfied. Each region has the shape of a cylindrical shell and the top and bottom surfaces of the cylinder are parallel to each other. This turns out to be a good approximation for those regions that are close to the axis of symmetry. The cylindrical shells are filled with a liquid crystal film, which is oriented by homeotropic surface boundary conditions. The height of the region, h_n, increases with increasing distance from the axis of symmetry as $h_n=\sqrt{R^2-r_n^2}+d$. Here R is the radius of the spherical surface, d is the separation between the flat surface and the sphere, whereas $r_n=R/2[\sin n\varphi-\sin(n-1)\varphi]$ is the distance between the central part of the n region and the axis of symmetry. Angle φ

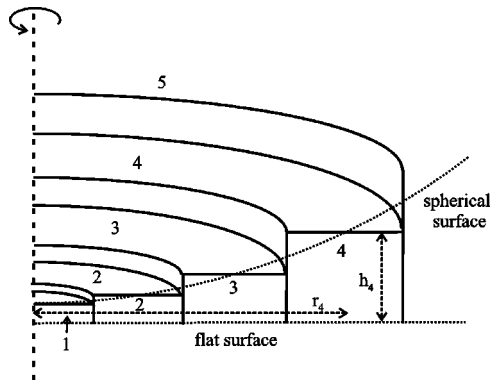

FIG. 5. Liquid crystal, which is filling the gap between the spherical and flat surfaces, is divided into a series of shells; each of them having a form of a thin liquid crystal film. The cross section of the model structure is presented together with parameters r_4 and h_4.

equals 360° divided by the number of polygons N. By choosing $N=72$, φ has a suitable value of 5° and the length of each polygon line equals 440 nm.

As shown in the study of liquid crystal properties in thin planar liquid crystal films [4,8], the interaction decreases approximately exponentially with increasing surfaces separation at temperatures above the nematic capillary condensation. For a typical nematic liquid crystal, the corresponding nematic correlation length is of the order of 10 nm at temperatures very close to the phase transition. Therefore, only those regions of model structure (Fig. 5) that are close to the symmetry axes are expected to have a significant contribution to the interaction mediated by the liquid crystal. In our calculations regions 1 to 9 are taken into account.

1. Properties of thin nematic films at temperatures above T_{NI}

The theoretical study, which comments the experimentally observed structural forces presented in the experimental section, is based on a mean-field calculation published in Ref. [8]. Here we only make a brief description of the model structure and present the most important conclusions.

A thin nematic film, which is a building block of our model structure, is confined between two parallel plates immersed in the isotropic phase of a nematic liquid crystal as shown schematically in Fig. 6. We assume that surfaces induce homeotropic anchoring, i.e., a perpendicular orientation of the molecules with respect to the surface. Homeotropic anchoring and the simple geometry of the system make the director field perpendicular to the surface everywhere in the film. The ordering of the liquid crystal in the film can therefore be reasonably described by a scalar order parameter S, which varies in the direction perpendicular to the plates (coordinate x).

The minimization of the Landau free energy functional yields a differential equation for the scalar order parameter (for details see Ref. [8]). Its solution, the order parameter profile $S(x)$, decreases approximately exponentially with the distance from the surface. The basic properties of $S(x)$ for the following values of material constants, which describe 8CB-like materials $a=0.18\times10^6$ J/m^3 K, $b=-2.3\times10^6$ J/m^3, $c=5.02\times10^6$ J/m^3, $L_1=3\times10^{-12}$ J/m, $T^*=312.5$ K [28], and surface coupling parameters set to $G=1\times10^{-3}$ J/m^2, $Q_s=0.3$ are presented below.

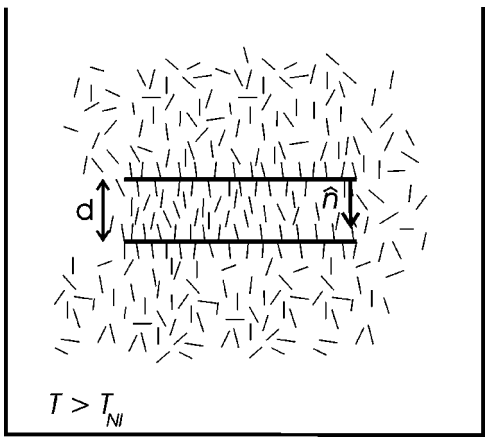

FIG. 6. A thin nematic film is confined between two large parallel plates immersed in an isotropic liquid crystal. The anchoring of molecules on surfaces is homeotropic, which induces a spatially uniform director field ($\hat{n}$) perpendicular to the surface.

(a). Stable and metastable phases. In the vicinity of T_{NI}, two different order parameter profiles minimize the free energy functional. One of the profiles corresponds to $S\sim0$ and describes the isotropic phase with a partial, surface-induced order, whereas the other one, having $S\sim0.3$, corresponds to the nematic phase. The lower value of the free energy defines a *stable phase* whereas the other phase is *metastable*. However, at the phase transition, both phases, the nematic as well as the partially ordered isotropic phase, ''cost'' the same amount of free energy. Since the appearance of the stable and metastable phases plays an important role in the explanation of our experiment, we illustrate this phenomenon in Fig. 7. The spatial dependence of the order parameter $S(x)$, which corresponds to the nematic phase, is shown in Fig. 7(a). Figure 7(b) presents order parameter profiles describing the partially condensed isotropic phase. To determine stability and metastability of order parameter profiles in Figs. 7(a) and 7(b), Fig. 7(c) depicts the free energy of the liquid crystal film per unit area for profiles shown in Figs. 7(a) and 7(b).

(b). Structural forces. Surface-induced orientational ordering above T_{NI} mediates forces between surfaces, which were first studied theoretically by Poniewierski and Sluckin [5]. As the origin of these forces is in the structure of the confined liquid, these are traditionally called ''structural forces'' [1]. Here we summarize relevant details of our investigation published in Ref. [8].

Structural forces are calculated by differentiating free energy of the system with respect to the separation between the surfaces. Since in thin nematic films with parallel boundaries forces are always perpendicular to the substrates, their direction can be sufficiently described with their signs. The negative values of the force correspond to an attraction, while the positive values indicate a repulsion.

To illustrate how the film thickness influences the magnitude of the structural force, mediated by the liquid crystal,

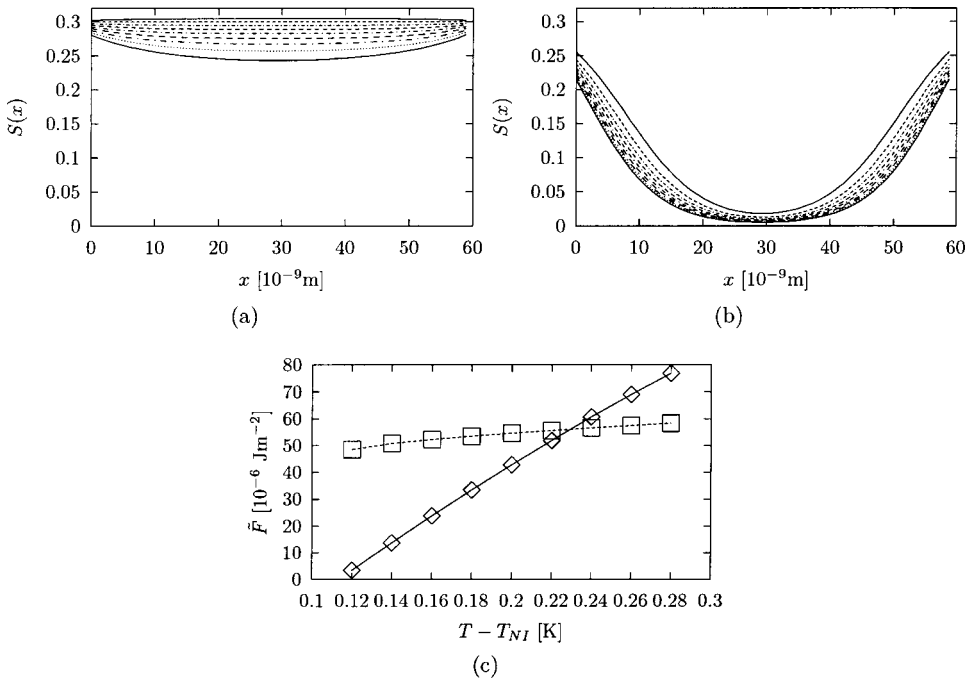

FIG. 7. Profiles of the scalar order parameter S in a thin nematic film. Temperatures: $T_{NI}+0.12$ K, $T_{NI}+0.14$ K, $T_{NI}+0.16$ K, $T_{NI}+0.18$ K, $T_{NI}+0.2$ K, $T_{NI}+0.22$ K, $T_{NI}+0.24$ K, $T_{NI}+0.26$ K, $T_{NI}+0.28$ K (from top to bottom). (a) Order parameter profiles that describe the nematic phase. (b) Order parameter profiles corresponding to the isotropic phase. (c) Free energy of the liquid crystal per unit area $\tilde{F}$ for profiles shown in (a) and (b); nematic phase→full line, isotropic phase→dashed line. Dots identify temperature values used in (a) and (b).

we show in Fig. 8 force per surface area as a function of film thickness for three different temperatures: $T_{NI}+0.28$ K, $T_{NI}+0.3$ K, and $T_{NI}+0.32$ K.

In Fig. 8(a) one can see that for thick films ($d>100$ nm) there is practically no structural force, which indicates that the liquid crystal can only be found in the isotropic phase. As the film thickness is reduced below the critical thickness ($d<95$ nm), the system can be found in a metastable, capillary condensed nematic phase as well. This results in two different force plots, stable isotropic (full line) and metastable and capillary condensed nematic (dashed line). For even thinner films ($d<47$ nm), the isotropic phase becomes metastable; whereas the capillary condensed nematic phase becomes stable. This is the point of phase transition. Below this value of film thickness, again two different values of force can be observed, one being metastable and close to zero (isotropic phase marked with dashed line) and the other one stable and of the order of 1×10^3 N m^{-2} (nematic phase marked with full line). For the particular selection of liquid crystal parameters, the attractive force due to capillary condensate is separation independent and equals 1.8×10^3 N m^{-2}. The fact that structural force due to capillary condensation is independent of separation indicates that it is exclusively a volume effect. This can be easily understood, as the free energy density difference between the nematic and isotropic phases is proportional to the confined volume of liquid crystal.

In Fig. 8(b) the occurrence of the stable and metastable phases and the possible values of force, depending on temperature, are shown. As the temperature is increased, the so-called *critical* film thickness, above which the system can be found in the isotropic phase only and therefore no force can be detected, decreases with temperature. As the temperature is raised from $T_{NI}+0.28$ K to $T_{NI}+0.32$ K, the film thickness is reduced from 92 to 45 nm.

2. Structural force mediated by a series of thin liquid crystal films

In this section we will show how to calculate the capillary force mediated by the liquid crystal film between a flat sur-

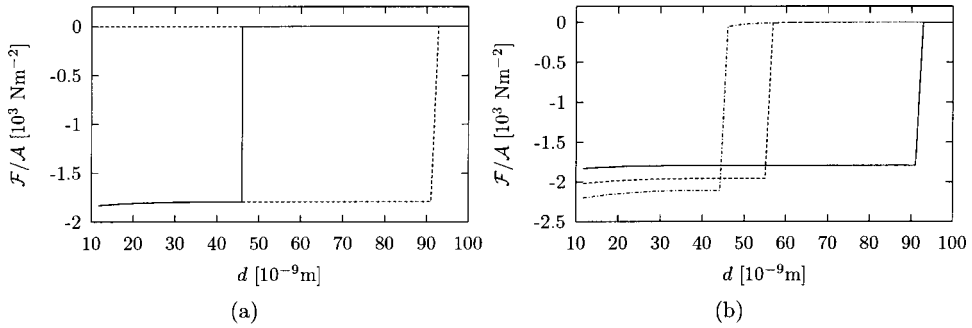

FIG. 8. Structural force per unit area as a function of separation between the plates. (a) $T=T_{NI}+0.28$ K, structural force corresponding to stable solution is marked by a full line and metastable by a dashed line. (b) Values of force corresponding to the nematic phase (stable or metastable) for three different temperatures: $T=T_{NI}+0.28$ K (full line), $T=T_{NI}+0.3$ K (dashed line), $T=T_{NI}+0.32$ K (dash-dotted line).

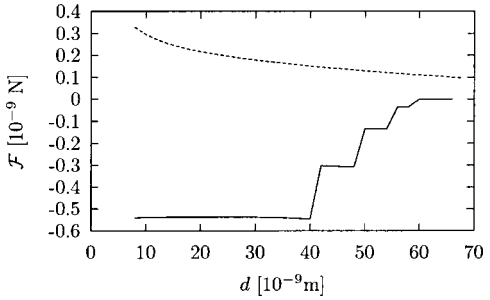

FIG. 9. Force between the flat surface and the sphere mediated by liquid crystal as a function of separation between the surfaces d (full line) and electrostatic repulsion as a function of d (dashed line). The temperature of liquid crystal is set to $T_{NI}+0.27$ K, whereas parameters, which determine the electrostatic repulsion, are equal to $p=0.13$, $\lambda_D=52$ nm, $\Psi_o=0.211$ V, $\delta=2.2\times10^{-5}$ As/m^2.

face and a sphere. The force is obtained as a sum of contributions corresponding to regions 1 to 9 presented in Fig. 5.

The contribution of each particular shell depends on the force per surface area, as well as on the volume of each cell. The volume of the cell increases with increasing distance from the symmetry axis, whereas the force per surface area decreases with increasing distance from the symmetry axis, as shown in Fig. 8. We would like to stress that completely different values of orientational order and the resulting forces in the neighboring liquid crystal shells can be understood in the context of structural domains.

In the experiment a small temperature gradient was observed in the liquid crystal filling the volume between the flat surface and the sphere. The temperature difference between the part of liquid crystal located at the symmetry axis of the system and that which is a few micrometers away was of the order of 0.01 K. This temperature gradient was also included in our model by simply setting the temperature in each particular shell to the appropriate value.

In Fig. 9 we illustrate how force mediated by a thin nematic film (full line) depends on surface separation. The temperature of the liquid crystal is set to $T_{NI}+0.27$ K. As one can see, the capillary force is nearly constant for low surface separation, $d<40$ nm, and vanishes at $d\approx60$ nm. We would like to stress that the discontinuities in the force profile, which appear at 40, 50, 56, and 60 nm, are due to the small number of shells considered in our model structure. If the liquid crystal film was described by a larger number of concentric shells, the force curve would be smoother as well.

B. Electrostatic repulsion

Surfaces of particles, which are immersed in liquid crystal, may become charged due to surface adsorption or dissociation of ions [1,29]. As shown in our recent experimental study [23], the resulting electrostatic interaction is an approximately exponentially decaying repulsion with the characteristic length of the order of 50 nm.

Here we consider the electrostatic repulsion as a superposition of two approximate solutions of the Poisson-Boltzmann equation, constant surface potential $\mathcal{F}^{cp}$ and constant surface charge approximation $\mathcal{F}^{cc}$ [30],

$$\mathcal{F}_e=p\mathcal{F}^{cc}+(1-p)\mathcal{F}^{cp}. \tag{1}$$

The two approximate solutions $\mathcal{F}^{cc}$ and $\mathcal{F}^{cp}$, on the other hand, are derived within the so called Derjaguin approximation and yield [29]

$$\mathcal{F}^{cc}=\frac{2\pi}{\epsilon\epsilon_o}R\lambda_D\delta^2\frac{\exp(-d/\lambda_D)}{1-\exp(-d/\lambda_D)}, \tag{2}$$

and

$$\mathcal{F}^{cp}=2\pi\epsilon\epsilon_o\frac{R}{\lambda_D}\Psi_o^2\frac{\exp(-d/\lambda_D)}{1+\exp(-d/\lambda_D)}. \tag{3}$$

Here λ_D is the Debye length, whereas Ψ_o and δ are the surface potential and surface charge density, respectively. Parameter ϵ is the dielectric constant of nematic liquid crystal and is taken to be 11 [31]. R is the radius of the sphere and d is the surface separation.

We would like to stress that expressions (2) and (3) are derived for two spherical surfaces in the limit $\lambda_D\ll R$, while in our experimental setup only one of the surfaces is curved whereas the other one is flat. However, our additional approximation can be justified by taking into account that, in our case, $d\ll R$ as well as $\lambda_D\ll R$, which makes both surfaces flat in comparison to the film thickness.

The electrostatic repulsion is illustrated in Fig. 9 (dashed line) with parameters p, λ_D, Ψ_o, and δ equal to 0.13, 52 nm, 0.211 V, and 2.2×10^{-5} Asm^{-2}, respectively. As one can see, the electrostatic force decays approximately exponentially with increasing film thickness. For this particular selection of parameters it has the same magnitude as the liquid crystal attraction which is also shown in Fig. 9.

When describing interactions that are mediated by the liquid crystal confined between a flat surface and a sphere, one should also mention the direct van der Waals interaction between the sphere and the substrate and pseudo-Casimir fluctuation force. As shown in the theoretical study of interactions between particles immersed in an isotropic liquid crystal [9], van der Waals interaction in the case of nearly refractive index matching conditions only presents a minor correction to the electrostatic and liquid crystal mediated interaction. The estimates of pseudo-Casimir force show that except in some particular cases it is negligibly small compared to mean field forces.

C. Comparison of theoretical prediction with experimental data

Following the theoretical approach presented above, we will now explain the basic properties of the experimentally determined force mediated by a partially ordered liquid crystal film. We consider a sum of the liquid crystal mediated structural force described in Sec. III A 2 and electrostatic repulsion, Sec. III B.

(a). Hysteresis loop. We first concentrate on two different values of force that can be observed for a particular selection of film thickness and temperature. The force profile obtained

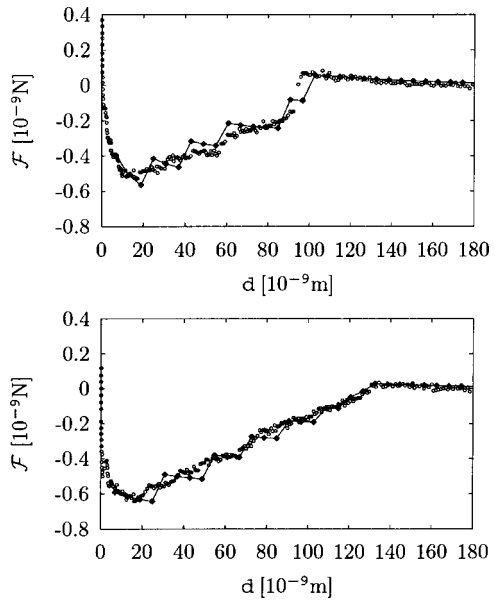

FIG. 10. Experimentally determined force (dots) compared to the theoretical prediction (diamonds). Top, sphere was approaching flat surface; bottom, retraction of the sphere. $T=40.956\,^{\circ}$C. Parameters for theoretical prediction: $p=0.13$, $\lambda_D=52$ nm, $\Psi_o=0.21$ V, $\delta=2.2\times10^{-5}$ Asm^2.

by approaching the surfaces is definitely different from that obtained by separating the surfaces. In Fig. 10 we show experimentally obtained force (dots) as a function of surface separation compared to the theoretical prediction (diamonds). The latter is a sum of liquid crystal mediated attraction and electrostatic repulsion, which are both presented in Fig. 9. The upper curve in Fig. 10 shows the force during the approach of the surfaces, whereas the lower curve describes the reverse situation. The two curves together form a kind of a *hysteresis loop*, which can be explained in terms of the stable and metastable phases introduced in Figs. 7 and 8 as follows. If the surface separation d is of the order of 100 nm or more, liquid crystal mediated attraction is negligible compared to the electrostatic repulsion. When the surface separation is reduced, liquid crystal remains in the stable isotropic phase even though its ordering could also be changed to the metastable nematic phase. If d is reduced even further, it reaches the point of phase transition where the nematic phase becomes stable and isotropic metastable (d_{pt}). At this point, the nematic phase capillary condenses for separation d that is smaller than d_{pt} and the liquid crystal ordering is changed from metastable isotropic to stable nematic phase. This results in a discontinuous appearance of an attractive force due to liquid crystal condensation. In Fig. 10 this transition appears at $d\approx95$ nm.

If, on the other hand, the initial surface separation is small, the liquid crystal is in the stable nematic phase. When separation d is increased beyond d_{pt}, the liquid crystal still remains in the metastable nematic phase, until the nematic phase disappears. As a result, the force between the surfaces remains attractive also at larger surface separations, where there is no force, if we initially start from the isotropic phase.

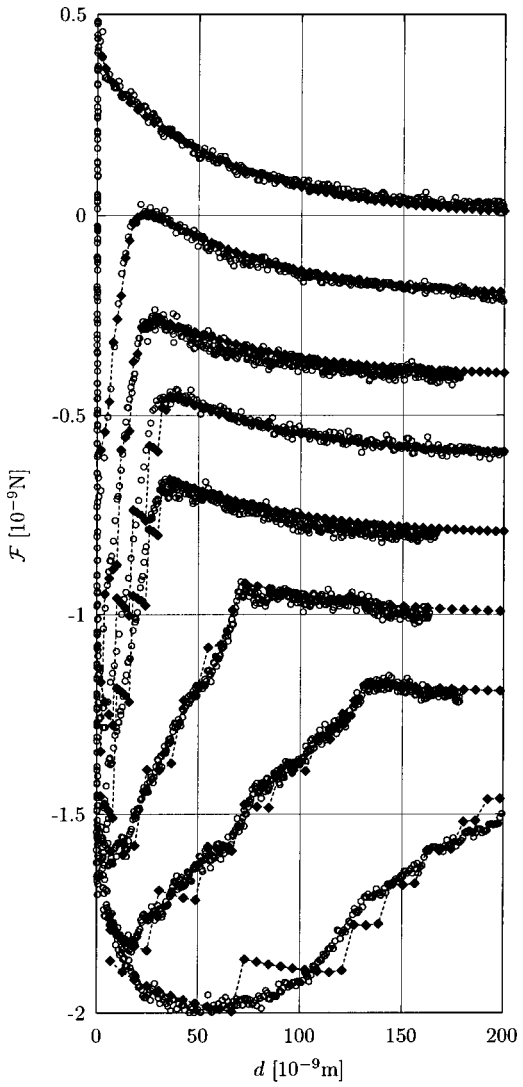

FIG. 11. Experimentally determined force (circles) compared to theoretical prediction (diamonds) at different temperatures: $T=41.26\,^{\circ}$C, $41.173\,^{\circ}$C, $41.1\,^{\circ}$C, $41.063\,^{\circ}$C, $41.051\,^{\circ}$C, $40.98\,^{\circ}$C, $40.956\,^{\circ}$C, $40.942\,^{\circ}$C (from top to bottom). All force curves are obtained during increasing surface separation. Parameters determining the electrostatic interaction are $p=0.13$, $\lambda_D=52$ nm, $\Psi_o=0.21$ V, $\delta=2.2\times10^{-5}$ Asm^2.

(b). Temperature dependence. In Fig. 11 we show how strongly is the interaction, mediated by the liquid crystal, influenced by the temperature. The eight force plots experimentally determined at different temperatures could be very well fitted to the theoretical predictions, using a single set of parameters and only changing the temperature from $40.9\,^{\circ}$C up to $41.3\,^{\circ}$C. The force profiles were obtained during increasing surface separation.

The force plot corresponding to the highest temperature $41.26\,^{\circ}$C (top curve) is repulsive in the whole interval of separations. The theoretical fit reveals that at this temperature the liquid crystal mediated attraction is negligible in comparison with electrostatic repulsion. As the temperature is reduced for 0.087 K (curve 2), the contribution of the liquid crystal becomes important at surface separations smaller than 20 nm. A further reduction of temperature ex-

pands the influence of liquid crystal to larger and larger separations. At the lowest temperature of our interest, 40.942 °C, it is dominating for surface separations d up to 180 nm.

IV. CONCLUSION

In this paper we have presented results of our atomic force microscope experiments, where a capillary condensation of a nematic liquid crystal was induced by precisely controlling the separation between the confining surfaces. We have detected an onset of strong capillary attractive forces over extraordinary large surface separations of several hundreds of nanometers, when the liquid crystal was close to the isotropic-nematic bulk phase transition. The measured force profiles were analyzed within the Landau–de Gennes approach, where also the surface charging was considered. We find a very good quantitative agreement between the experiment and theory, which is also reflected in the fact that a single set of parameters is needed to describe the measured forces in the temperature range of observation. Equally important, the analysis of our force experiments clearly shows that the Landau–de Gennes theory of structural forces in nematic liquid crystals is valid down to the nanoscale level.

[1] J. Israelachvili, *Intermolecular and Surface Forces* (Academic Press, New York, 1992).
[2] W.T.T.L. Kelvin, Philos. Mag. **42**, 448 (1871).
[3] P. Sheng, Phys. Rev. Lett. **37**, 1059 (1976).
[4] P. Sheng, Phys. Rev. A **26**, 1610 (1982).
[5] A. Poniewierski and T.J. Sluckin, Liq. Cryst. **2**, 281 (1987).
[6] P. Poulin, V. Cabuil, and D.A. Weitz, Phys. Rev. Lett. **79**, 4862 (1997).
[7] T.C. Lubensky, D. Pettey, N. Currier, and H. Stark, Phys. Rev. E **57**, 610 (1998).
[8] A. Borštnik and S. Žumer, Phys. Rev. E **56**, 3021 (1997).
[9] A. Borštnik, H. Stark, and S. Žumer, Phys. Rev. E **60**, 4210 (1999).
[10] H. Stark, Phys. Rep. **351**, 387 (2001).
[11] K. Kočevar, A. Borštnik, I. Muševič, and S. Žumer, Phys. Rev. Lett. **86**, 5914 (2001).
[12] K. Miyano, Phys. Rev. Lett. **43**, 51 (1979).
[13] J.C. Tarczon and K. Miyano, Phys. Rev. Lett. **46**, 119 (1981).
[14] H. Yokoyama, S. Kobayashi, and H. Kamei, Appl. Phys. Lett. **41**, 438 (1982).
[15] H. Yokoyama, J. Chem. Soc., Faraday Trans. 1 **84**, 1023 (1988).
[16] H. Yokoyama, *Handbook of Liquid Crystal Research* (Oxford University Press, Oxford, 1997), Chap. 6.
[17] M. Wittebrood, Ph.D. thesis, University of Nijmegen, 1997.
[18] A. Golemme, S. Žumer, D.W. Allender, and J.W. Doane, Phys. Rev. Lett. **61**, 2937 (1988).
[19] K. Kočevar and I. Muševič, Phys. Rev. E **65**, 021703 (2002).
[20] K. Kočevar and I. Muševič, Phys. Rev. E **64**, 051711 (2001).
[21] F.J. Kahn, G.N. Taylor, and H. Schonhorn, Proc. IEEE **61**, 823 (1973).
[22] J.Y. Huang, R. Superfine, and Y.R. Shen, Phys. Rev. A **42**, 3660 (1990).
[23] K. Kočevar and I. Muševič, Phys. Rev. E **65**, 030703 (2002).
[24] R.A. Orwoll, V.J. Sullivan, and G.C. Campbell, Mol. Cryst. Liq. Cryst. **149**, 121 (1987).
[25] A.J. Leadbetter, J.L.A. Durrant, and M. Rugman, Mol. Cryst. Liq. Cryst. **34**, 231 (1977).
[26] S. Faetti and V. Palleschi, Phys. Rev. A **30**, 3241 (1984).
[27] C.S. Park, N.A. Clark, and R.D. Noble, Phys. Rev. Lett. **72**, 1838 (1994).
[28] H.J. Coles, Mol. Cryst. Liq. Cryst. **49**, 67 (1978).
[29] W.B. Russel, D.A. Seville, and W.R. Schowalter, *Colloidal Dispersions* (Cambridge University Press, Cambridge, 1995).
[30] S.H. Behrens and M. Borkovec, J. Phys. Chem. B **103**, 2918 (1999).
[31] R.G. Horn, J. Phys. (France) **39**, 105 (1978).